Geological Survey of Canada

CURRENT RESEARCH
2003-C14

Teleseismic investigations of the lithosphere beneath central Baffin Island, Nunavut

D. Snyder

2003

CURRENT RESEARCH

Natural Resources Canada Ressources naturelles Canada

Canada

ISSN 1701-4387
Catalogue No. M44-2003/C14E-IN
ISBN 0-662-33536-8

A copy of this publication is also available for reference by depository libraries across Canada through access to the Depository Services Program's website at http://dsp-psd.pwgsc.gc.ca

A free digital download of this publication is available from the Geological Survey of Canada Bookstore web site:

http://gsc.nrcan.gc.ca/bookstore/

Click on Free Download.

Author's address

D. Snyder (dsnyder@nrcan.gc.ca)
Geological Survey of Canada
615 Booth Street
Ottawa, Ontario K1A 0E9

Publication approved by Continental Geoscience Division

Teleseismic investigations of the lithosphere beneath central Baffin Island, Nunavut

D. Snyder

Snyder, D., 2003: Teleseismic investigations of the lithosphere beneath central Baffin Island, Nunavut; Geological Survey of Canada, Current Research 2003-C14, 8 p.

Abstract: From summer 2000 to summer 2002, five self-contained seismic stations were established and operated on central Baffin Island to study the lithospheric structure across the Proterozoic–Archean boundary, the northern margin of Trans-Hudson Orogen. Crustal thickness estimates decrease steadily from 40 (±2) km in the southeast to 37 (±2) km beneath the Archean block in the northwest. Prominent southward-dipping mantle discontinuities occur beneath the southeasternmost stations at about 100 and 140 km depth, defining a layer of increased seismic velocity. Crustal discontinuities occur at 2 and 15 km depths beneath these stations. Two layers with differing anisotropic properties are also indicated in the south from observed azimuthal variations in the splitting of teleseismic SKS-waves: probable axes of anisotropy strike at 82° and 41°. In the north, neither clear discontinuities nor anisotropy are observed, suggesting a heterogeneous lithosphere.

Résumé : De l'été 2000 à l'été 2002, cinq stations sismiques autonomes ont été installées et mises en service dans l'île de Baffin centrale afin d'étudier la structure de la lithosphère de part et d'autre de la limite Protérozoïque-Archéen, qui forme la marge nord de l'orogène trans-hudsonien. Les épaisseurs crustales estimées décroissent régulièrement de 40 (±2) km dans le sud-est à 37 (±2) km sous le bloc archéen au nord-ouest. Sous les stations les plus au sud-est, des discontinuités proéminentes à pendage sud sont présentes dans le manteau à des profondeurs de 100 et 140 km environ, où elles définissent une couche de plus grande vitesse sismique. Des discontinuités dans la croûte sont observées à 2 et 15 km sous ces stations. Dans le sud, on déduit également l'existence de de deux couches ayant des propriétés anisotropes différentes d'après les variations azimutales observées dans le déphasage des ondes télésismiques SKS : les axes probables de l'anisotropie sont dirigés à 82° et 41°. Aucune discontinuité évidente ni anisotropie ne sont observées dans le nord, ce qui laisse croire à l'hétérogénéité de la lithosphère.

INTRODUCTION

In order to provide three-dimensional (depth) information for a regional mapping project on central Baffin Island, Nunavut (Fig. 1) (Corrigan et al., 2001; Scott et al., 2002), we installed a number of self-powered teleseismic stations for year-round operation in this remote northern setting. These stations are passive recorders of seismic waves generated by distant (teleseismic) earthquakes worldwide.

Herein we report initial results from the five sites located in central Baffin Island, Nunavut (Fig. 1). This work is one part of a multi-disciplinary, joint GSC and Canada-Nunavut Geoscience Office, four-dimensional, regional geoscientific study of central Baffin Island, Nunavut (St-Onge et al., 2002a, b). The acquisition of these data provided valuable information about equipment design, logistical support, and cost of acquisition in such remote areas. The analysis described here uses two well established techniques for data from single, independent stations and targets seismic-wave property anisotropy (foliation) and near-horizontal discontinuities in seismic properties of the rocks throughout the lithosphere beneath the station and down to depths greater than 450 km.

DATA ACQUISITION

Government and university geophysicists have used the seismic station design used in this study for at least 5 years. The sensor is the CMG-40T model made by Guralp Systems in the United Kingdom. Its functional bandwidth is rated as 50 Hz to 30 s and it is a passive-feedback, three-component seismometer. The recorder is the Orion built by Nanometrics, Inc. in Kanata, Ontario. The recorder stores the data in digital format in memory and automatically downloads these data to a removable hard disk every 0.5 to 6 hours. The two-gigabyte disks used typically can store 180 to 270 days worth of three-component data and state-of-health information. The sampling rate used is 20 samples/s.

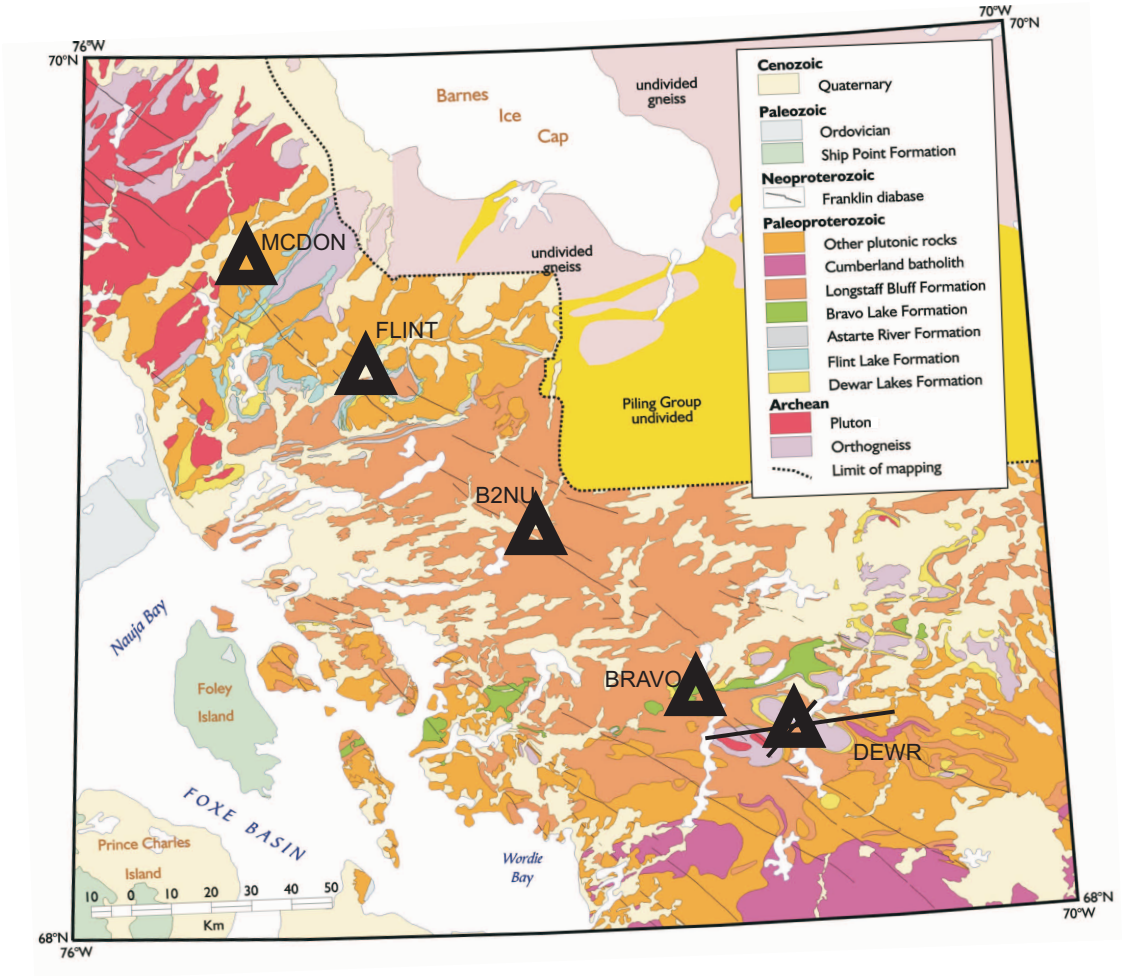

Figure 1. *Location map for the central Baffin teleseismic stations; base is the project's geological compilation map (St-Onge et al., 2002b). Triangles mark locations of the teleseismic stations used in this study. The bars at station DEWR show the directions of anisotropy modelled in two layers beneath the station.*

Table 1. Location and operating period for temporary stations on central Baffin Island used in this study.

Station	Lat. (°N)	Long. (°E)	Start	End	Days
DEWR	68.4619	-71.588	23-Jul-00	16-Aug-02	719
BRAVO	68.5492	-72.1385	6-Jul-01	16-Aug-02	267
B2NU	68.9216	-73.1973	21-Jul-00	23-Dec-00	152
FLINT	69.293	-74.197	8-Jul-01	14-Aug-02	140
MCDON	69.5199	-74.9084	10-Jul-01	15-Aug-02	222

Seismic stations were installed out of the GSC's Central Baffin base camp in July 2000 and 2001 (Table 1). The remote location required that the stations be visited only twice each year, in April and during the summer. Equipment failure, flooding of the vault, and wildlife damage could only be identified and repaired at those times. Some stations performed well; DEWR recorded 96% of the 25 month period it was deployed, whereas, B2NU recorded only 20% (5 months) over that same period. Only one or two stations recorded many of the useful earthquakes (Table 2).

DISCONTINUITY STUDIES

Two types of analytical techniques were applied to these data. The first, the so-called 'receiver function' method (e.g. Ammon et al., 1990; Bostock, 1998), provides identification of major discontinuities in seismic velocity or density within the lithosphere. Recorded signals represent the convolution of the source signature with the Earth filter (its internal structure). To obtain the Earth structure, the source signature must be deconvolved from the recorded signal. In the deconvolution version applied here (Bostock, 1998), the primary S-wave arrival is compared to the primary P-wave arrival in order to estimate the source signature, which is then removed. The resulting Earth filter is typically expressed as a series of discontinuities below the recording station. The Moho is very often the most prominent discontinuity observed (e.g. Ramesh et al., 2002) and the clarity of its resolution provides a good calibration on the quality of the data recorded. As with all seismic methods, the greater the number of earthquake-station pairs, the better the resolution of the analysis. This method produces robust estimates with tens of such pairs, typically acquired over 4 to 12 months. It is thus possible to determine major discontinuities in the crust and mantle beneath each of the five stations of this study. The results beneath station DEWR are the most reliable and are discussed first.

Twenty-four months of recording produced 37 earthquakes useful for receiver-function analysis at station DEWR (Table 2). These functions show systematic variations depending on the azimuth from which the seismic energy arrives (typically called the "back azimuth", BAz) and it is therefore useful to group them into sectors to improve the signal. For DEWR, 20 earthquakes were grouped in the northwest sector (270–359°) at great circle arc distances of 30° to 99°. The deconvolution results for 16 of the best northwestern events (Fig. 2) show a clear Moho discontinuity at 41 km on the radial component and a prominent negative contrast discontinuity on both components at about 145 km depth. Another eight earthquakes formed an S sector group (175–215°).

Table 2. Earthquakes used for receiver function analysis.

Earthquake location	Date	Time	BAz	D	Station
Japan	30-Jul-00	12:25:45	332	75	G
Sakhalin Is.	04-Aug-00	9:13:02	335	60	G D
Bonin Island	06-Aug-00	7:27:12	333	80	G D
Mexico	09-Aug-00	11:41:47	217	54	G D
Ecuador	28-Sep-00	23:23:43	187	69	G
Japan	27-0ct-00	4:21:51	330	82	G
Kodiak	06-Nov-00	11:40:26	293	35	G D
Panama	08-Nov-00	6:59:59	187	62	G D
Alaska	29-Nov-00	10:25:13	300	28	G
Nicaragua	04-Dec-00	4:43:09	206	56	G D
Caspian	06-Dec-00	5:11:06	42	65	G
El Salvador	13-Jan-01	17:33:32	200	56	D
India	26-Jan-01	3:16:40	35	84	
Oregon	28-Feb-01	6:54:32	210	25	D
Japan	24-Mar-01	6:27:53	339	76	D
Japan	14-Apr-01	23:26:00	331	79	D
Japan	25-May-01	0:40:50	329	64	D
Aleutians	14-Jun-01	19:48:47	308	49	D
Peru	23-Jun-01	20:33:14	182	85	D
Peru	26-Jun-01	4:18:31	180	86	D
Marianas	03-Jul-01	13:10:42	328	87	D
Peru	07-Jul-01	9:38:43	181	86	D
Aleut	28-Jul-01	7:32:43	297	35	D M F
Aleut	02-Aug-01	23:41:06	320	48	B M F
Japan	13-Aug-01	20:11:23	332	68	D M B F
Alaska	14-Sep-01	4:45:08	260	33	B M F
Kamchatka	08-Oct-01	18:14:26	321	52	B M F
Kuriles	09-Oct-01	23:53:37	325	59	D B M F
Marianas	12-Oct-01	15:02:16	322	94	D M B F
Banda	19-Oct-01	3:28:44	301	108	M B F
China	14-Nov-01	9:26:10	343	78	D M B F
Tajikistan	23-Nov-01	20:43:00	306	72	D
Japan	02-Dec-01	13:01:53	334	70	D
Taiwan	18-Dec-01	4:02:58	347	87	D
Hindu Kush	03-Jan-02	7:05:27	31	72	D
Russia/China	01-Feb-02	21:55:20	338	64	D
Hindu Kush	03-Mar-02	12:08:22	32	72	D
Japan	26-Mar-02	3:45:49	346	88	D
Taiwan	31-Mar-02	6:52:51	347	87	D
Kamchatka	26-Apr-02	7:15:11	323	52	D B
Marianas	26-Apr-02	16:06:07	324	94	D B
Kamchatka	08-May-02	19:45:18	323	52	B
Alaska	25-May-02	5:36:31	296	41	D B M
Japan	03-Jun-02	9:15:00	330	80	D M
SW Pacific	10-Jun-02	22:48:36	328	97	D M
Iran	22-Jun-02	2:58:21	342	67	D B M
Russia/China	28-Jun-02	17:19:30	342	67	D B M
Oregon	09-Jul-02	18:40:34	258	38	M
Japan	02-Aug-02	23:11:39	333	78	D M
Panama	07-Aug-02	23:59:14	188	62	

BAz is the back azimuth, the direction pointing back to the earthquake from DEWR; D is the distance in degrees between DEWR and the earthquake; G = B1NU; D = DEWR; B = BRAVO; M = MCDON; F = FLINT

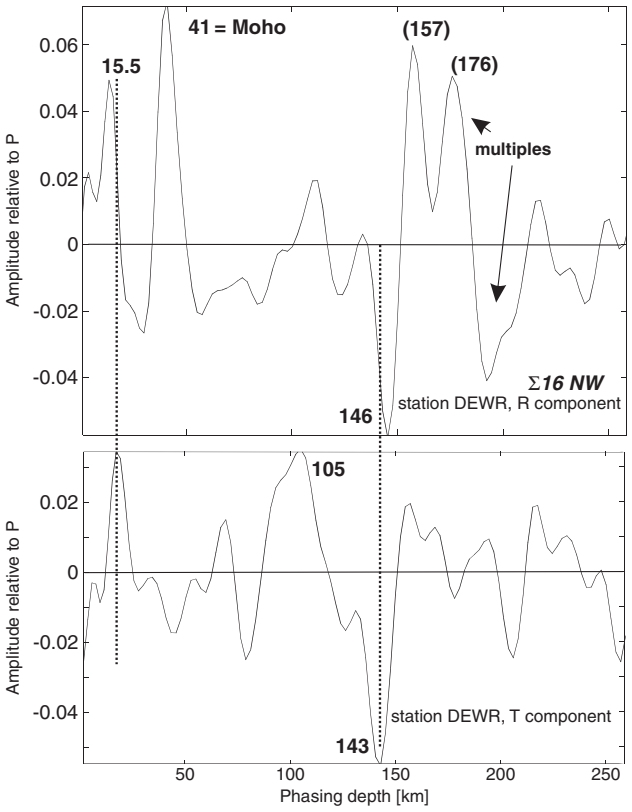

Figure 2. *Plots of cross-correlation amplitudes relative to P-wave arrival versus depth for station DEWR. Depth conversions assumed a standard lithosphere model for all stations. Here, 16 teleseismic earthquakes, all located northwest of the station, were analyzed simultaneously. The radial component (R) is shown at the top, the transverse (T) component, at the bottom. Numbers are in kilometres and indicate depth to major seismic discontinuities (some are reverberations or multiples). The Moho is most clearly observed on the R component; deeper discontinuities are best observed on the T component.*

These showed a Moho at 41 km and a negative discontinuity at 74 km depth on the radial component; significant positive and negative features occur at 90 to 125 km on the transverse component.

In order to estimate the depth to discontinuities, a standard velocity model (iasp91: Kennett and Engdahl, 1991) for continental areas was assumed to convert the delay times that are actually measured. Velocity variation with depth can also be modelled directly from the data (Fig. 3) (Darbyshire, in press). Beneath DEWR, the Moho is consistently modelled at 40 to 42 km depth, an unusually thick crust. Velocity models for events arriving from the south in particular show layers of relatively low velocity within the crust, varying from 10 to 25 km depths, but strong variations at this depth are observed to the northwest also (Fig. 2, 3). This station is on a gneiss dome of Archean basement rock, so these layers are not sedimentary and probably lie below crystalline upper crust, possibly related to Paleoproterozoic tectonics or intrusions associated with the Trans-Hudson Orogen.

The shorter recording window at the other four stations results in fewer useful earthquakes, but happily most of those recorded arrived within the same northwestern sector and provide a means to compare results from all the stations, using the results from DEWR as a control or basis for comparison. Fourteen earthquakes arriving within the northwest quadrant at the BRAVO station revealed discontinuities very consistent with those observed at the nearby DEWR station (Fig. 4). Notable are a Moho at 39 km and discontinuities on the transverse component at 100, 143, and 164 km depths.

Events from all azimuths were jointly deconvolved to produce the receiver functions for station B2NU (GSC base camp) (Fig. 4). A Moho at 40 km and a minor discontinuity at 172 km are the only significant features. Farther north, eight useable earthquakes from the northwest recorded at the station on FLINT Lake revealed a Moho at 39 km and shallow mantle discontinuities at depths of 57 to 65 km, but none deeper (Fig. 5). At station MCDON, the Moho is at 37 km depth and minor mantle discontinuities with negative downward contrasts occur at 44, 65, 107, and 213 km on either the radial or transverse component (Fig. 5).

ANISOTROPY STUDIES

The second analytical tool again draws heavily upon results from the station DEWR. Estimates of lithospheric-scale foliation using anisotropy of SKS seismic phases (e.g. Silver, 1996) are neither as numerous nor as consistent as the deconvolution results because of the limited periods of recording at most stations.

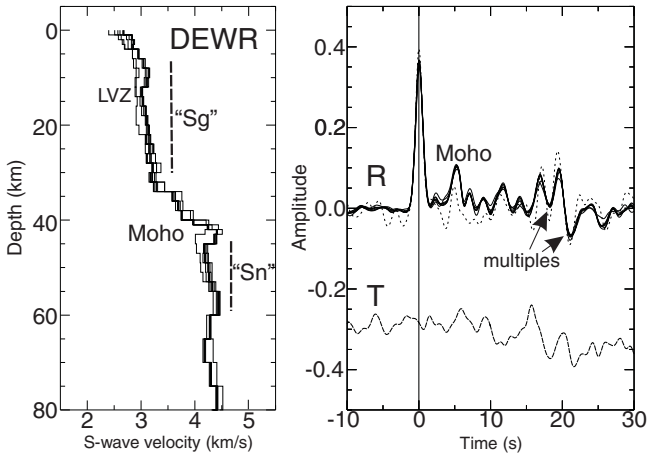

Figure 3. *Plots of one-dimensional velocity–depth models (left) and resulting (dotted lines) versus observed (solid lines) cross-correlation values (right) for station DEWR. Model results courtesy of F. Darbyshire (2002). Note the distinct increase in velocity associated with the Moho and resulting primary and multiple spikes on the cross-correlation trace. Vertical bars on the one-dimensional model represent S-wave velocities expected on the basis of the regional velocity analysis (*see *Fig. 8). LVZ is a crustal low-velocity zone noted by Darbyshire (in press); Sg, typical velocity within the crust; Sn, typical velocity within the upper mantle.*

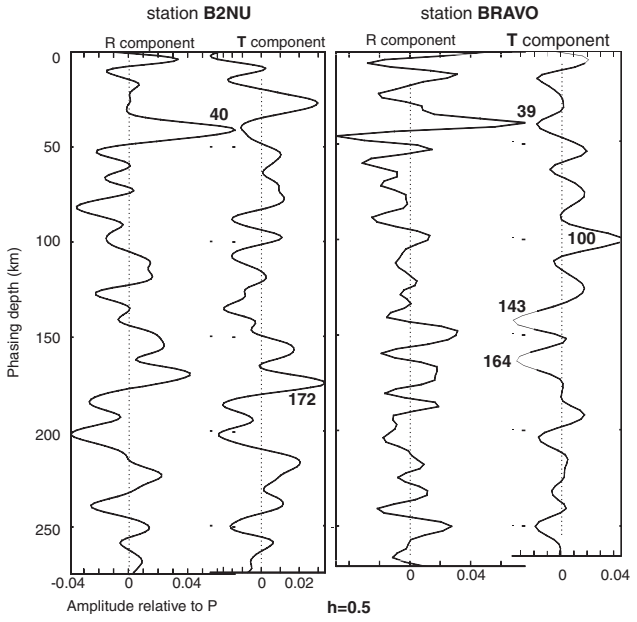

Figure 4. *Plots of cross-correlation amplitudes relative to P-wave arrival versus depth for stations B2NU (GSC camp) and BRAVO; labels as in Figure 3. B2NU analysis used 11 earthquakes from all azimuths; BRAVO used 14 earthquakes from the northwest quadrant. Functions were smoothed using a Gaussian parameter, h = 0.5.*

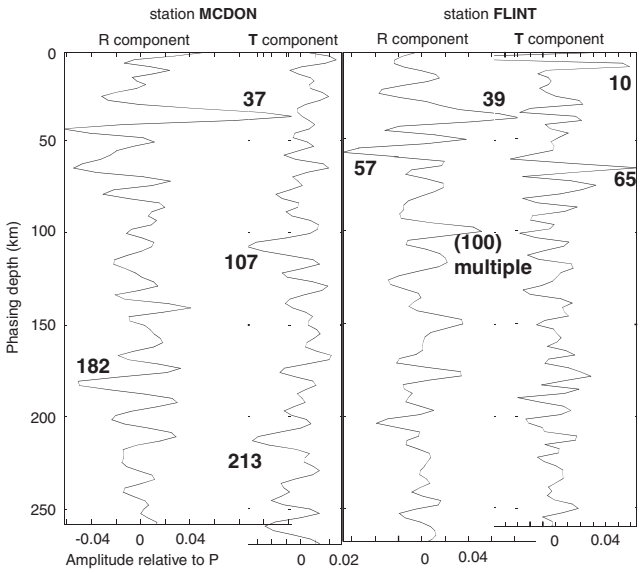

Figure 5. *Plots of cross-correlation amplitudes relative to P-wave arrival versus depth for stations MCDON and FLINT; labels as in Figure 3. MCDON analysis used 16 earthquakes from the northwest quadrant; FLINT used 8 earthquakes from the northwest quadrant. Functions were smoothed using a Gaussian parameter, h = 0.75.*

Table 3. Earthquakes used for anisotropy studies at the DEWR site.

Event	Δ	BAz	ϕ(°)	±	dt (s)	±	Station	Earthquake location
28aug00 15:05	114	339	2	5	1.80	0.45	D	Papua N. Guinea
			93	9	0.85	0.24	G	
4oct00 16:58	115	294	57	13	1.20	0.25	D	N. Hebrides
27oct00 04:21	82	331	48	11	0.90	0.30	D	Izu/Japan (387 km)
			57	8	0.93	0.15	G	
7nov00 00:18	127	151	108	9	1.05	0.25	D	Scotia Arc
			100	6	2.13	0.39	G	
18dec00 01:19	116	278	44	22	0.50	0.40	D	Fiji
1jan01 06:57	103	341	173	23	1.05	1.45 N	D	Phillipines
9jan01 16:49	115	294	57	5	0.65	0.10	D	N. Hebrides
13feb01 19:28	116	7	31	23	0.65	0.65	D	Sumatra
28apr01 04:48	112	277	46	9	0.45	0.10	D	Kermadec
11sep01 14:56	109	331	26	17	0.65	0.30	B	Irian Jaya
12oct01 0502	94	322	67	23	0.65	0.45	D	Marianas
			77	14	0.55	0.23	M	
19oct01 03:28	114	340	72	6	1.90	0.45	D	Banda Sea
			101	15	0.80	0.30	M	
31oct01 09:10	110	314	72	6	1.10	0.18	D	New Britain
2jan02 17:22	117	292	50	23	0.65	0.85	D	Vanuatu
5mar02 11:15	105	344	69	23	2.95	3.54 N	D	Philippines
26mar02 03:45	88	346	83	23	0.95	2.45 N	D	Japan
28mar02 04:56	90	177	49	23	0.45	0.90	D	Chile
31mar02 06:52	87	347	88	23	0.90	2.08 N	D	Taiwan
18apr02 16:08	96	179	16	23	0.55	0.55	D	Chile
26apr02 16:06	95	325	62	10	1.00	0.53	D	Marianas
28may02 04:04	97	176	56	12	0.60	0.20	D	Argentina
17jun02 21:26	113	296	56	14	0.70	0.25	D	St. Cruz Islands
18jun02 13:56	99	179	19	23	0.75	0.75	D	Chile
27jun02 05:50	119	5	38	23	0.70	0.95 N?	D	Sumatra
30jun02 21:29	117	279	53	8	0.55	0.10	D (B)	Fiji

Event is the date and time (hour:minute) of the earthquake considered. Δ is the distance in degrees between DEWR and the earthquake; BAz is the back azimuth, the direction pointing back to the earthquake from DEWR; ϕ is the fast apparent anisotropy direction; dt is the delay or splitting time; N indicates a poorly constrained solution, possibly a null result because anisotropy and back azimuth directions coincide.

Estimates of shear-wave splitting were made using SKS and SKKS phases from 24 teleseismic earthquakes recorded at station DEWR, whereas at most three earthquakes could be used at any of the other four stations (Table 3). Mode conversion at the core–mantle boundary ideally removes source side anisotropy effects and produces a radially polarized S-wave at the core–mantle boundary. The methodology of Silver and Chan (1991) was used to model splitting of individual shear waves; this method assumes that the lithosphere is a homogeneous and weakly anisotropic medium. In this medium, nearly vertical S-wave propagation is characterized by ϕ, the azimuth of the shear-wave polarization with maximum velocity, and *dt*, the accumulated arrival time difference between fast and slow polarizations. Analysis consists of finding values of ϕ and *dt* that best convert the observed elliptical particle motion to a linear, radial particle motion. These assumptions require ϕ and *dt* to show no variation with back azimuth, the direction to the earthquake from the station.

Anisotropy at DEWR shows a consistent variation with back azimuth (Fig. 6). The pattern observed is suggestive, on the basis of numerous synthetic models and theory (Silver and Savage, 1994; Saltzer et al., 2000), of two distinct layers, each with a different anisotropy. Least-squares fitting of a modelled variation with back azimuth to the observations indicates that a lower, thicker layer has a nearly east-west (082°) fast polarization azimuth. Note the back azimuth where the minimum occurs in the predictive model results (Fig. 6). A shallower layer with one-fourth the amount of anisotropy has a northeast-southwest (041°) fast polarization azimuth. Total delay times vary between 0.45 and 1.9 s with an average of 0.84 ± 0.5 s, indicating moderately strong anisotropy beneath DEWR.

Many of the earthquakes producing clear SKS splitting at DEWR did not produce similarly consistent results at other stations. Estimates with unreasonably large values of delay times or uncertainties or unusual fast polarization angles often cluster near a specific back azimuth. The two-layer modelling indicates that this is expected at 'nodes', where back azimuth coincides with fast polarization or lies 90° from it. This is an important feature of the two-layer model at DEWR; note the cluster of nodal values (N) in Figure 6. These erratic values can also signify either a lack of anisotropy or complexly layered anisotropy (e.g. Saltzer et al., 2000), and this is probably the case beneath stations MCDON and FLINT where statistically significant groups (5–10) of strong earthquakes produced no consistent results, as noted above.

REGIONAL VELOCITY ESTIMATES

Regional earthquakes at 100 to 2000 km distances can provide important information about crustal and uppermost mantle velocities in the study area, using predominantly horizontally propagating seismic waves. This vertical velocity resolution is not directly available from traditional teleseismic data analysis because it uses predominantly vertically propagating waves. Four teleseismic stations recorded earthquakes with hypocenters located in oceanic areas surrounding Baffin Island in autumn 2001 (Fig. 7; Table 4). Travel times of the first P-wave arrivals were plotted against distance in order to determine the seismic wave velocities (Fig. 8). A single crustal velocity (Pg phase) of 6.36 km/s was measured, as was an uppermost mantle velocity (Pn phase) of 8.38 km/s. The crustal velocity is poorly constrained, particularly at near offsets. These appear somewhat high when compared with the mean S-wave velocities of 3.2 and 4.25 km/s determined from the one-dimensional inversion of receiver functions at station DEWR (Fig. 3), assuming typical Vp/Vs of 1.76 to 1.80 (e.g. Bostock, 1998).

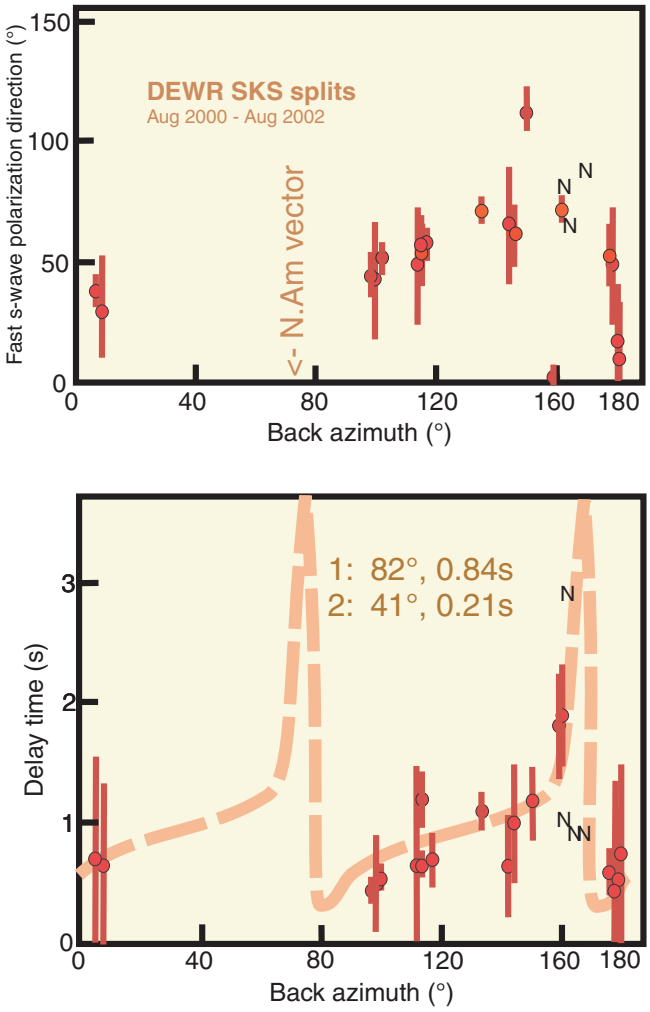

Figure 6. *Plots of the variation of the direction of the fast axis of polarization and of the delay time between radial and transverse components of the S-waves with back azimuth direction toward the earthquake. The data and uncertainties plotted here are listed in Table 1. Values repeat every 180°. N indicates a probable nodal response that typically occurs when the anisotropy fast or slow axis coincides with back azimuth direction. The dashed line represents the distribution expected from a two-layer model of anisotropy with the parameters indicated. The regional North America Plate motion direction is also shown.*

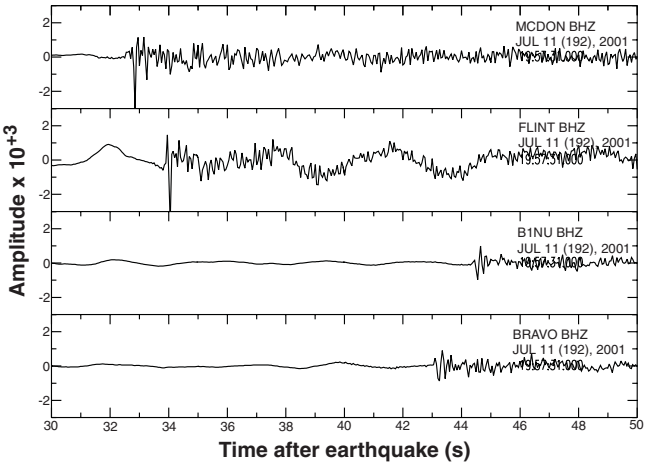

Figure 7. *Regional earthquake on 11 July 2001 (*see *Table 3) recorded at four of the stations and used to estimate average crust and uppermost mantle velocities.*

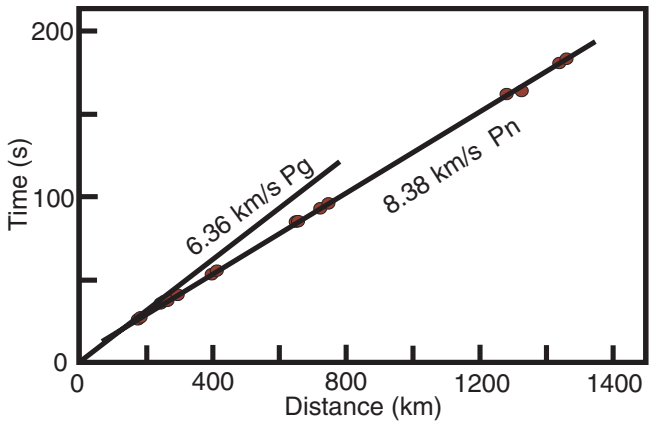

Figure 8. *Plot of arrival time versus distance between earthquake and seismic station for four regional earthquakes (*see *Table 3). The Pg phase travels within the crust; the Pn phase travels within the uppermost mantle.*

PRELIMINARY INTERPRETATIONS

The teleseismic observations described herein provide low-resolution, but clear indications of variations in mantle structure beneath central Baffin Island (Fig. 9). Beneath the Proterozoic–Archean crustal boundary at stations DEWR and BRAVO, strong seismic discontinuities occur at about 100 and 145 km depths bounding a layer of increased seismic velocity. The top of this layer may dip northwestward to 175 km depth beneath the centre of the Proterozoic basin; it may also deepen to the south beyond the area studied. The mantle beneath DEWR is also characterized by two distinct layers of anisotropy, and a reasonable inference is that the observed discontinuities also represent anisotropy layer boundaries. The mantle discontinuities at 100 and 145 km are defined primarily by relatively strong seismic-wave arrivals on the transverse components (Fig. 2, 4). In theory, seismic energy arrives on this component only if layers are anisotropic or heterogeneous in their seismic properties; fossil or active subducted slabs are common sources of such mantle

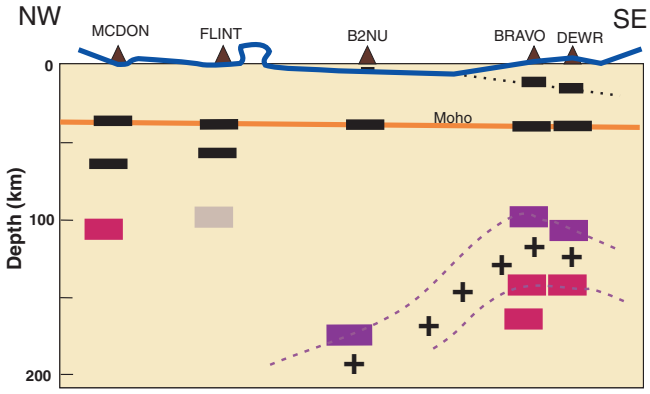

Figure 9. *Cross-section of the lithosphere beneath central Baffin Island as constrained by the teleseismic results described herein. A major boundary in the mantle appears to lie just northwest of station BRAVO. Plus signs indicate a layer with increased S-wave propagation velocities. The solid (blue) line at the top is the mapped basement–cover boundary, dated at ca. 2.15 Ga.*

Table 4. Location and origin time of earthquakes used in regional velocity study. Under each station are shown the travel time and the distance between earthquake and the station.

Origin Time	Lat (°N) Long. (°E)	Mag	MCDON	FLIN	BRAV	DEWR
11jul2001	71.01	3.3	32.4s	33.9s	43.1s	44.2s
19:57:31	71.69		206km	214 km	275km	284km
17jul2001	62.67	3.8	99.3s	96.7s	89.5s	89.4s
02:09:44	75.62		764km	741	675km	672km
14aug2001	76.63	5.6	162s	163s	181s	183s
19:35:38	107.16		1324km	1287km	1440km	1461km
14sep2001	72.13	3.6	43.7s	46.9s	58.7s	60.8s
21:20:42	75.75		293km	322km	422km	438km

anisotropy (e.g. Bostock, 1998). Thus, the two independent analysis tools applied to the central Baffin teleseismic data point toward a similar conclusion: a layered mantle, possibly a rift or continental convergent margin, lies approximately below the mapped trace of the Bravo Lakes Formation and the Proterozoic–Archean boundary zone in the southern segment of the study area (St-Onge et al., 2002b).

Farther north the crust is thinner and no clearly defined mantle structure is observed. Anisotropy results are notably inconclusive and mantle discontinuities are of low amplitude and do not correlate strongly between stations. These, albeit negative, characteristics are typical of some Archean shield areas (e.g. Silver, 1996) and are thus consistent with current interpretation of this northern part of the central Baffin field area. This suggests that the Proterozoic Piling Group (St-Onge, 2002a) was deposited along the southern (current co-ordinates) passive margin of the Archean Rae Craton and was subsequently deformed by tectonism occurring farther outboard.

Within the crust, discontinuities are observed at depths of 10, 4, 14, and 16 km, beneath stations FLINT, B2NU, BRAVO, and DEWR, respectively. The 4 km depth is similar to estimates of depth to top of crystalline basement determined from down-dip projection of surface bedrock mapping (F. Berniolles, unpub. data, 2002). The increases in velocity associated with the deeper boundaries to the south may represent the bottom of a low-velocity layer or the top of a high-velocity layer. If the former, unusually thick Piling Group metaturbidite units were possibly stacked and underthrust to these depths. If the latter, sills and dykes feeding the Bravo Lakes Formation mafic extrusives may have also intruded the middle crust.

A nearly coincident magnetotelluric transect (Jones et al., 2002) provides independent observations supporting these interpretations. The preliminary magnetotelluric model contained robust indications of 1) a major break in crustal conductivity near teleseismic stations DEWR and BRAVO, 2) strong vertical conductivity gradients between 35 and 40 km depths beneath stations MCDON, FLINT, and B2NU, contrasting with weaker gradients between 40 and 55 km beneath DEWR and BRAVO, and 3) implied more resistive mantle at 50 to 120 km depths in the north than in the south. The overall impression is of a different lithospheric column beneath the Dewar Lakes area, in the southern segment of the Proterozoic–Archean boundary zone, compared with mapped Archean regions to the north. This is consistent with the results from the teleseismic analysis.

REFERENCES

Ammon, C.J., Randall, G.E., and Zandt, G.
1990: On the nonuniqueness of receiver function inversions; Journal of Geophysical Research, v. 95, p. 15 303–15 318.

Bostock, M.G.
1998: Mantle stratigraphy and evolution of the Slave Province; Journal of Geophysical Research, v. 103, p. 21 183–21 200.

Corrigan, D., Scott, D.J., and St-Onge, M.R.
2001: Geology of the northern margin of the Trans-Hudson Orogen (Foxe Fold Belt), central Baffin Island, Nunavut; Geological Survey of Canada, Current Research 2001-C23, 11 p.

Darbyshire, F.A.
in press: Crustal structure across the Canadian High Arctic region from teleseimsic receiver function analysis; Geophysical Journal International.

Jones, A.G., Spratt, J., and Evans, S.
2002: Central Baffin electromagnetic experiment (CBEX); Geological Survey of Canada, Current Research 2002-C19, 5 p.

Kennett, B.L.N. and Engdahl, E.R.
1991: Traveltimes for global earthquake location and phase identification; Geophysical Journal International, v. 105, p. 429–465.

Ramesh, D.S., Kind, R., and Yuan, X.
2002: Receiver function analysis of the North American crust; Geophysical Journal International, v. 150, p. 91–108.

Saltzer, R.L., Gaherty, J.B., Jordan, T.H.
2000: How are vertical shear wave splitting measurements affected by variations in the orientation of azimuthal anisotropy with depth?; Geophysical Journal International, v. 141, p. 374–390.

Scott, D.J., St-Onge, M.R., and Corrigan, D.
2002: Geology of the Paleoproterozoic Piling Group and underlying Archean gneiss, central Baffin Island, Nunavut; Geological Survey of Canada, Current Research 2002-C17, 10 p.

Silver, P.G.
1996: Seismic anisotropy beneath the continents: probing the depths of geology; Annual Review of Earth and Planetary Sciences, v. 24, p. 385–432.

Silver, P.G. and Chan, W.W.
1991: Shear wave splitting and subcontinental mantle deformation; Journal Geophysical Research, v. 96, p. 16 429–16 454.

Silver, P.G. and Savage, M.K.
1994: The interpretation of shear wave splitting parameters in the presence of two anisotropic layers; Geophysical Journal International, v. 119, p. 949–963.

St-Onge, M.R., Scott, D.J., and Corrigan, D.
2002a: Geology, Inuksulik Lake, Nunavut; Geological Survey of Canada, Open File 4317, scale 1:250 000 (paper and CD-ROM versions).
2002b: Geology, Dewar Lakes, Nunavut; Geological Survey of Canada, Open File 4201, scale 1:100 000 (paper and CD-ROM versions).

Geological Survey of Canada Project PS1006